University of Groningen

Irradiation of isolated collagen mimetic peptides by x rays and carbon ions at the Bragg-peak energy

Lalande, M.; Abdelmouleh, M.; Ryszka, M.; Vizcaino, V.; Rangama, J.; Mery, A.; Durante, F.; Schlatholter, T.; Poully, J-C

IMPORTANT NOTE: You are advised to consult the publisher's version (publisher's PDF) if you wish to cite from it. Please check the document version below.

Document Version
Publisher's PDF, also known as Version of record

[Link to publication in University of Groningen/UMCG research database](#)

Irradiation of isolated collagen mimetic peptides by x rays and carbon ions at the Bragg-peak energy

M. Lalande,[1] M. Abdelmouleh,[1] M. Ryszka,[1] V. Vizcaino,[1] J. Rangama,[1]
A. Méry,[1] F. Durantel,[1] T. Schlathölter,[2] and J.-C. Poully[1,*]

[1]*CIMAP, UMR 6252 (CEA/CNRS/ENSICAEN/Université de Caen Normandie), Caen, France*
[2]*Zernike Institute for Advanced Materials, University of Groningen, Nijenborgh 4, 9747AG Groningen, Netherlands*

We report on an experimental irradiation of isolated peptides by carbon ions at the Bragg-peak energy. Collagen mimetic peptides and their noncovalent complexes undergo nondissociative ionization, but also inter- and intramolecular fragmentation induced by internal energy transfer. We also detect nondissociative proton detachment, an ion-specific process. The average amount of energy transferred by ions is similar to the case of x-ray single photoabsorption, and our results indicate that it changes with the conformation and size of a given molecular system. Our work paves the way to experimental investigation of high-energy ion collisions involving proteins and DNA strands, to investigate the role of ion kinetic energy in internal energy deposition.

I. INTRODUCTION

Effects of ionizing radiation on matter have been studied for more than 100 years, in particular by William and Lawrence Bragg during the late 19th to early 20th centuries. The former discovered that charged particles (notably ions) with MeV kinetic energies penetrate into matter and deposit energy along a mostly linear path, making them decelerate and stop at a depth that increases with initial kinetic energy. Along this path, the linear energy transfer (LET) is first almost constant, and then shows the so-called Bragg peak right before the particles stop. This LET is mainly due to ionization of atoms and molecules along the ion path, and the Bragg peak can be accounted for by the evolution of electronic stopping power while ions are decelerated. Hadrontherapy for cancer treatment (mainly with protons but also carbon ions) takes advantage of this ion-specific interaction with matter to maximize energy deposition in tumors and spare healthy tissues located along the ion path, especially deeper than the Bragg-peak location. This precise ballistics adds to a higher relative biological efficiency than conventional treatments to kill cancer cells [1]. Cell death may occur following DNA strand break, either by direct interaction with the primary beam or by indirect effects such as radical attacks after water radiolysis and interaction with secondary particles [2]. However, fundamental molecular processes underlying these biological effects are still poorly understood. Several groups have tackled this task by studying the irradiation of isolated biologically relevant systems, starting with building blocks of DNA, proteins, and lipids in a bottom-up approach. DNA bases [3–7], nucleosides [8–11] and nucleotides [12], amino acids [13–16], small peptides [17,18], and carbohydrates [12,19,20] have been ionized mainly by photons but also electrons and ions. Moreover, the role of a molecular surrounding on the

ionization and fragmentation of these small molecules within clusters has been probed [21–24]. Only recently, soft sources of gas-phase molecules allowed irradiation of larger systems such as proteins [25,26] and DNA strands [27] stored in ion traps. However, only a few papers report on ion collision with a protein [28–30].

Collagen is the most abundant protein in the human body, its triple-helix structure (see Fig. 1) being responsible for the mechanical properties of many tissues (skin, bones, cartilage, nails, etc.). Recently, we showed that protonated peptide trimers known to be model systems of this triple helix keep their condensed-phase structure in the absence of a solvent, but only for charge states higher than 7 [31]. In this work, we present the results of experimental collisions between collagen mimetic triple-helix models and ions at the Bragg-peak energy (≈ 1 MeV/u). These $((PPG)_{10})_3$ and $((PHypG)_{10})_3$ triple-helix models consist of three noncovalently bound peptides, each consisting of ten repetitions of the sequence proline-proline-glycine or its hydroxylated form proline-hydroxyproline-glycine. We use mass spectrometry for analyzing the main processes induced, but also for estimating the internal energy transferred to the molecular system, thanks to comparison with the results of x-ray photoabsorption experiments.

II. EXPERIMENTAL SECTION

All experiments were performed using a homemade tandem mass spectrometer that has been described in detail somewhere else [33] and is shown in Fig. 2. Briefly, molecules are put in the gas phase thanks to an electrospray ion source (ESI) and guided through a funnel and an octopole. The molecule of interest is then selected by its mass over charge ratio (m/z) in a quadrupole mass spectrometer (QMS), before being accumulated in a Paul trap and irradiated by the ion or photon beam. All trapped cations are then extracted and analyzed in a time-of-flight (TOF) mass spectrometer before

FIG. 1. Structure of the collagen triple-helix peptidic model $((PPG)_{10})_3$ (Protein Data Bank ID: 1K6F [32]). Backbones are shown as ribbons, with one color for each peptide.

being detected by a microchannel plate (MCP) detector. For the spectra shown in Fig. 3, the latter consisted of one MCP, a scintillator, and a photomultiplier (Bipolar TOF, Photonis). This allowed a postacceleration voltage of -9.0 kV to be applied to the front MCP, and thus increased detection efficiency compared to MCP detectors alone (–5.0 kV), which were used in the case of the spectra shown in Fig. 4.

Irradiation with carbon ions was performed at the GANIL facility in Caen (France), by coupling the tandem mass spectrometer to the IRRSUD beamline. We used a C^{4+} ion beam at 0.98 MeV/u, with an intensity of 25 nA. The irradiation time was controlled by pulsing the carbon ion beam thanks to an electrostatic deflector located after the ion source, but before acceleration by the cyclotron. X-ray photon irradiation was carried out at the BESSYII synchrotron (U49/2-PGM1 beamline, HZB, Berlin, Germany), and a mechanical shutter was used to control the irradiation time. In both cases, the irradiation time was on the order of 500–1500 ms.

The $(PPG)_{10}$ and $(PHypG)_{10}$ collagen mimetic peptides were purchased from Peptides International (>95% purity) and used without further purification. Powders were dissolved in equal proportions of water and methanol, with 1% of formic acid in volume. The final concentration was around 50 μmol/l. For each molecular system studied, we recorded a mass spectrum without the ionizing beam (beam off), and two with the beam (beam on). We then subtracted the "beam off" spectrum from the average of the two "beam on" spectra. The result is a negative peak for the parent ion, and all positive peaks are products of the interaction involving a change in m/z. The resulting spectrum was smoothed by adjacent averaging over 20 points, and calibrated in m/z. Since the flux is about 10^{13} photons/s for x rays and 4×10^{10} ions/s for C^{4+}, photoabsorption or collision events are independent. Therefore, we tuned the irradiation time to induce less than
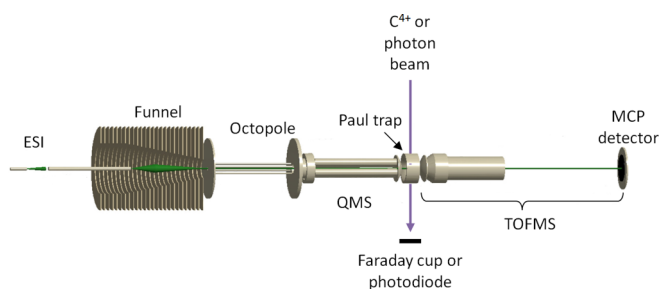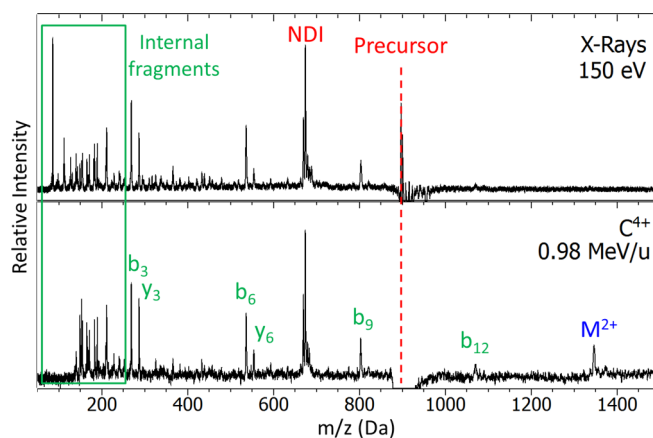

FIG. 2. Scheme of the experimental setup.

FIG. 3. Mass spectra of the $[(PHypG)_{10} + 3H]^{3+}$ peptide after irradiation by an x-ray beam at 150 eV (top) and the C^{4+} ion beam at 0.98 MeV/u (bottom). Red dashes indicate the precursor ion ($m/z = 898.0$); the corresponding peak appears negative as explained in the experimental section. NDI stands for nondissociative ionization, M^{2+} is the doubly protonated peptide ion, and b_{3n}/y_{3n} backbone fragment ions have been assigned. In the C^{4+} spectrum, no peaks appear below $m/z = 100$, due to the higher trap RF voltage and thus m/z cutoff.

10% depletion of the precursor ion: It ensures that our mass spectra contain more than 90% of events coming from single interactions. We also irradiated the trap residual gas without the molecular ion beam (by turning off the electrospray needle voltage) to spot background peaks.

Since the MCP detection efficiency depends on ion velocity and thus m/z, all ion yields determined from the mass
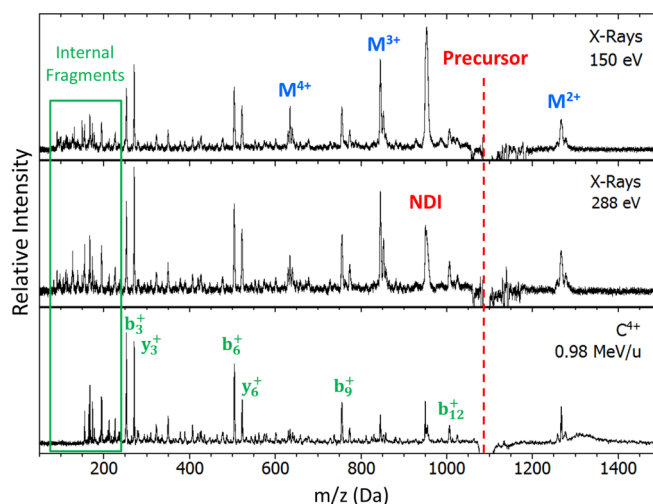
FIG. 4. Mass spectra of the $[((PPG)_{10})_3 + 7H]^{7+}$ trimer after irradiation by x rays at 150 and 288 eV as well as by C^{4+} ions. The position of the precursor ion ($m/z = 1085.7$) is represented by red dashes. Nondissociative ionization (NDI), monomers (M^{n+}) and the main backbone fragment ions (b_{3n}/y_{3n}) are indicated in red, blue, and green, respectively. In the C^{4+} spectrum, no peaks appear below $m/z = 100$, due to the higher trap RF voltage and thus m/z cutoff.

spectra and included in Figs. 5–7 were corrected by detector efficiency, with the same method as reported earlier [26].

III. RESULTS AND DISCUSSION

A. Irradiation of isolated collagen mimetic peptides

First, we present our results on isolated collagen mimetic peptides (monomers), before exploring the role of complexation in the next subsection, dedicated to peptide trimers. It is worth pointing out that we only present the results for the $(PHypG)_{10}$ peptide, since we obtained very similar ones for $(PPG)_{10}$. Figure 3 shows a comparison between mass spectra of the $[(PHypG)_{10} + 3H]^{3+}$ after irradiation by an x-ray photon beam at 150 eV, and by a C^{4+} ion beam at 0.98 MeV/u. The main observation is the striking similarity of the two spectra: For both, the main product cations are $[(PHypG)_{10} + 3H]^{4+}$ with $m/z = 673.5$, due to nondissociative ionization (NDI), and backbone fragments, as we recently reported [34]. The latter are mainly singly charged b_{3n} and y_{3n} ($1 \leqslant n \leqslant 4$ being a positive integer) fragments coming from glycine-proline peptide bond cleavages, but also b_2, y_2, b_4, y_5 and below $m/z = 250$, mainly internal fragments formed by at least two backbone cleavages. Regarding photoabsorption at 150 eV, this energy is far lower than the ones corresponding to the electronic transitions involving $1s$ electrons of C, N, and O atoms. The photon is thus absorbed by electrons of valence orbitals, one or several electrons are ejected, and the residual energy is redistributed in the vibrational modes of the peptide and leads to its fragmentation. On the other hand, carbon ions at 0.98 MeV/u are expected to interact with electrons of the molecule, located in mostly valence but also inner orbitals, as Tribedi *et al.* reported for collisions between C^{6+} ions at 3.5 MeV/u and uracil [35]. The similarity of the mass spectra for x rays and C^{4+} ions (cf. Fig. 3) indicates that both particles interact with electrons, eject at least one of them and deposit internal vibrational energy in the system. Later in this paper, we will give an upper limit to this amount of deposited energy.

The main processes induced by carbon ions and x-ray photons are the same, but a clear difference appears between the spectra of Fig. 3. A peak at $m/z = 1346.4$ corresponding to the $[(PHypG)_{10} + 2H]^{2+}$ peptide is visible only after carbon ion irradiation. We attribute this contribution to nondissociative proton detachment from the precursor ion. This phenomenon was never reported after photon irradiation, and has been observed for collisions between Xe^{8+} ions and multiply protonated cytochrome C [28]. It was demonstrated that the probability of proton detachment increases with the initial number of protons in the precursor ion. This is consistent with our results, since we irradiated the doubly protonated $[(PHypG)_{10} + 2H]^{2+}$ peptide with C^{4+} ions, but detected no proton detachment (data not shown). A relevant thermochemical property to consider for proton detachment is gas-phase acidity of a given molecular system M: it corresponds to the Gibbs free energy of the gas-phase reaction $[M + nH]^{n+} \rightarrow [M + (n-1)H]^{(n-1)+} + H^+$. It has been shown that the gas-phase acidity of peptides at 300 K increases with the number of protons, consistently with the previous and present results. Furthermore, typical values for gas-phase acidity range from 8 to 11 eV [36,37]: Since ionization energies of protonated peptides lie in the same

range [38], although slightly higher, it confirms the possible competition of proton detachment vs ionization.

B. Irradiation of collagen triple-helix models

1. X-ray photoabsorption

Compared to the isolated peptide monomers (cf. Fig. 3), we observe the same species in the mass spectra of protonated triple-helix models (see Fig. 4): the intact ionized peptide trimer due to NDI and backbone fragments. However, a noticeable difference is the presence of peaks assigned to peptide monomers with charge states 2+, 3+, and 4+. They are due to intermolecular dissociation of the triple helix, which is mainly composed of two M^{2+} and one M^{3+}, as we reported earlier [34]. Therefore, the observation of M^{4+} indicates nondissociative ionization of a M^{3+} within the triple helix, followed by dissociation into monomers. We previously reported that these peptide monomers can further undergo backbone cleavage if the photon energy is high enough, indicating that the amount of energy transferred to the system increases with photon energy [34].

Figure 5 presents the relative yields of NDI, monomers as well as backbone fragments of the collagen mimetic peptide triple helix $[((PPG)_{10})_3 + 7H]^{7+}$ after x-ray photoabsorption in the 100–535 eV energy range. Those relative yields are defined as a proportion of all irradiation products: $RY_i = \frac{A_i}{\sum A_i}$, where A_i is the absolute integrated area under the peak i. Note that areas are corrected by the detector efficiency factor. The observed trends are consistent with those already reported for the same system in the VUV-X range [34]. In comparison with VUV energies, fragmentation is the main contribution after x-ray photoabsorption, and globally increases with photon energy, confirming that the vibrational energy transferred to the system also rises. However, this evolution is far from linear, since all yields are mostly constant from 100 to 250 eV, and a sudden change occurs between 250 and 288–300 eV: NDI
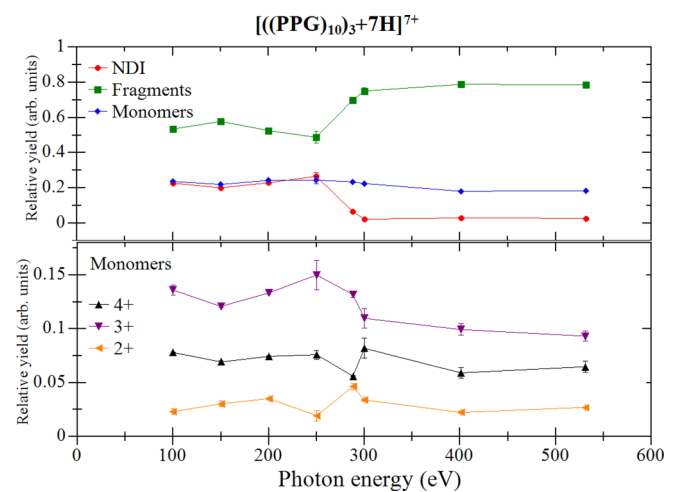

FIG. 5. Relative yields of nondissociative ionization (NDI), sum of monomers in 2+, 3+, and 4+ charge states, and backbone fragments of the $[((PPG)_{10})_3 + 7H]^{7+}$ trimer as a function of the absorbed x-ray photon energy. The evolution of the different charge states of the monomer is also shown in the bottom plot. Uncertainties come from the method used for data analysis.

strongly falls while backbone fragments follow the opposite trend, whereas the abundance of monomers remains almost constant. From 300 to 535 eV, yields are again constant. We attribute this behavior to the fact that for 288 eV and above, photoabsorption transfers more internal vibrational energy leading to backbone fragmentation of the peptide. Indeed, below 288 eV, only valence electrons can absorb the photon, whereas from 288 eV, electrons located in $1s$ atomic orbitals of C, N, and O are expected to be involved. Photoabsorption at 288, 401.5, and 531.5 eV is known to target C, N, and O $1s$ electrons, respectively, and induce resonant excitation to π^* orbitals of the amide groups of isolated peptides and proteins, followed by Auger electron emission [39], while the remaining electronic energy is converted into vibrational energy (about 20 eV on average for 288 eV [26]). At 300 eV, one C $1s$ electron is brought to the continuum, and one Auger electron is ejected, which results in double ionization and in a larger fragmentation yield compared to 288 eV [26]. This is consistent with our results, and they also indicate that photoabsorption by valence electrons deposits less vibrational energy than $1s$ electrons. Our previous study on a peptidic sequence of type I collagen led to the same conclusion [40]. Interestingly, the total yield of 2+, 3+, and 4+ monomers remains broadly constant over the whole energy range, which might be due to photoabsorption of valence electrons even at energies of 288 eV and above, the excess energy being carried away by the ejected electron. When looking at the bottom plot of Fig. 5, one can notice that from 288 to 300 eV, 2+ and 3+ charge state monomers slightly decrease while the 4+ rises: This is attributed to double ionization of a monomer 2+ within $[((PPG)_{10})_3 + 7H]^{7+}$, the latter being most likely composed of two monomers 2+ and one 3+.

To further characterize double ionization following single photoabsorption, we studied $[((PPG)_{10})_3 + 6H]^{6+}$ from 288 to 300 eV photon energy, with 1.5-eV steps. We chose this charge state because double ionization of the triple helix can be assigned unambiguously. On Fig. 6 the relative yields of fragments, NDI, NDDI (nondissociative double ionization), and monomers are plotted as a function of photon energy. Over the whole energy range, the main relaxation pathway is peptide backbone fragmentation, as for $[((PPG)_{10})_3 + 7H]^{7+}$ (cf. Fig. 5), and the second most abundant is intermolecular dissociation forming monomers. We can notice opposite trends between NDI and NDDI. While the yield of NDI is slowly decreasing between 288 and 300 eV, NDDI is constant from 288 to 294 eV, increases from 294 to 297 eV, and then is again constant. This trend was previously observed for cytochrome C by Milosavljevic *et al.* [39]. From 294 to 297 eV, peptide backbone fragmentation slightly decreases, while monomers increase in abundance, indicating that double ionization does not deposit enough internal energy to induce fragmentation of monomers formed by intermolecular dissociation. This is consistent with a transition from excitation to ionization in this photon energy range, as we reported recently for VUV photons on the same system [34].

2. X-ray photoabsorption vs **C⁴⁺** *irradiation spectra*

For each photon energy included in Fig. 5, we compared the mass spectra of the $[((PPG)_{10})_3 + 7H]^{7+}$ collagen triple-
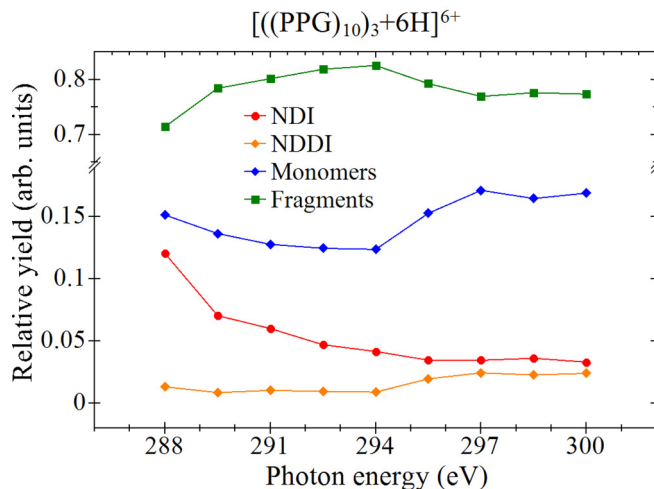

FIG. 6. Relative yields of nondissociative ionization (NDI) and double ionization (NDDI), sum of monomers in 3+ and 4+ charge states, and backbone fragments of the $[((PPG)_{10})_3 + 6H]^{6+}$ trimer as a function of the absorbed x-ray photon energy between 288 and 300 eV. The doubly charged monomer is not included since it has the same m/z as the precursor ion and thus cannot be detected.

helix model with the one obtained after carbon ion irradiation. The photon energy of 288 eV compares better to carbon (cf. Fig. 4). However, it is worth noting that the abundances of NDI and monomers, in comparison with backbone fragments, are smaller after carbon ion than photon irradiation. We will discuss this point more deeply in the next section. Interestingly, in the C⁴⁺ spectrum, the peak corresponding to M^{2+} is much more intense (taking into account detection efficiency) than M^{3+}, contrary to the case of x rays. This can be rationalized by the contribution of nondissociative proton detachment from $[((PPG)_{10})_3 + 7H]^{7+}$, giving $[((PPG)_{10})_3 + 6H]^{6+}$, as observed for isolated peptides (*vide infra*). Furthermore, it was unambiguously observed for other charge states of the peptide trimers. Besides, this process is less probable for trimers in 5+ and 6+ charge states than for the triply protonated monomers, which might be in contradiction with the simple picture of a process influenced by the number of protons alone, as proposed by Martin *et al.* [28]. However, another explanation could be a partial dissociation of the trimer into monomers, after proton detachment. It would imply that this process induces a certain amount of vibrational energy transfer.

3. Internal energy deposition by x rays and **C⁴⁺** *ions*

In the case of photons, we showed in the previous section that the amount of internal energy transferred to the molecular system can be tuned by changing their energy. In the case of ions, can this amount be varied and/or controlled?

First, let us consider how to calculate the stopping power of ions of a given kinetic energy in a given material in the condensed phase, thanks to the SRIM software [41]. For ^{12}C ions at 12 MeV in a polyimide of density 1.42 and containing H, C, N, and O, it gives about 90 eV/Å. Let us consider the diameter of a disk with an area equal to the collision cross section as an approximation of the ion path within the molecular system. We recently measured this cross section for low-
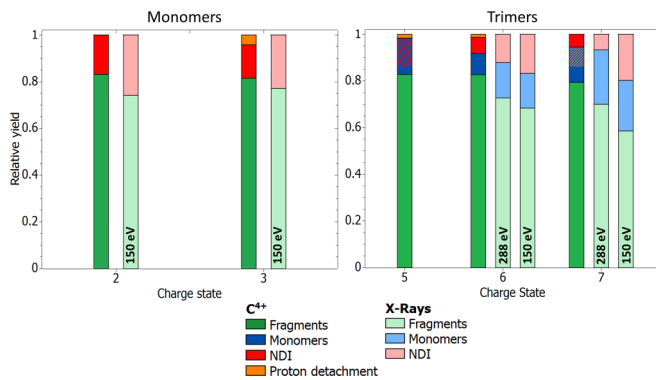
FIG. 7. Relative yields of NDI, fragments, monomers, and proton detachment after x-ray (150 eV for monomers, 150 and 288 eV for trimers) and carbon irradiation as a function of charge state. The results are highly similar for both $(PHypG)_{10}$ and $(PPG)_{10}$ monomers, we thus only show the data for $(PHypG)_{10}$, extracted from the spectra of Fig. 3. For $[((PPG)_{10})_3 + 5H]^{5+}$, NDI cannot be separated from M^{2+}; they both contribute to the sum of monomers. For $[((PPG)_{10})_3 + 6H]^{6+}$, the M^{2+} monomers formed by dissociation of the triple helix have the same m/z as the precursor ion, and thus do not contribute to the sum of monomers. Proton detachment from $[((PPG)_{10})_3 + 7H]^{7+}$ and M^{2+} have the same m/z; they both contribute to the sum of monomers.

energy collisions with He by ion-mobility spectrometry, and obtained values about 1400Å^2 for the $[((PPG)_{10})_3 + 7H]^{7+}$ trimer (corresponding to a triple helix shown in Fig. 1), and 425Å^2 for the doubly protonated $[PPG_{10} + 2H]^{2+}$ monomer (a folded structure) [31]. The ion path across the system would therefore be about 40 and 20 Å, corresponding to a transferred energy of around 3600 and 1800 eV for the trimer and monomer, respectively (note that the stopping power is constant over the path).

Second, it is useful to recall that by measuring the fragmentation yield of molecular systems in the gas phase, our collaboration reported previously that absorption of a photon of 288 eV transfers around 20 eV to the system [26]. In Fig. 7, we compare the fragmentation yields of collagen peptide monomers and trimers after x ray and irradiation by C^{4+} ions at 0.98 MeV/u. First, it is clear that these yields are hardly influenced by the charge state. Second, for trimers, they are similar for a photon energy of 288 eV: Therefore, C^{4+} ions at 0.98 MeV/u may transfer about 20 eV to the system. For monomers, the corresponding photon energy is 150 eV: Since it is lower than 288 eV, we showed in the previous section that the transferred energy is lower than 20 eV, but of the same order of magnitude. Therefore, it is around 100 times lower than what we estimated for the condensed phase in the previous paragraph: The main reason is most probably the kinetic energy carried away by the emitted electrons in our gas-phase experiments.

On the other hand, with x rays, a clear effect of stabilization via complexation is seen: For a photon energy of 150 eV, the amount of backbone fragmentation decreases from monomers to trimers. In our recent paper [34], we attributed this to, first, a size effect that allows distributing the transferred vibrational energy into about three times more degrees of freedom, and second, to evaporative cooling that dissipates energy by breaking the H bonds of the triple helix. The fact that we do not observe such an effect for carbon ion irradiation indicates that the stabilization effect via complexation is roughly canceled out by the increase in deposited energy due to the larger ion path within the system.

Unfolding, complexation, and change in the size of the system therefore influence the fragmentation yield after irradiation. If our interpretation is correct, the amount of vibrational energy transferred by the ion to a given molecular system can be increased by unfolding its structure. It also demonstrates the power of mass spectrometry in indirectly measuring this amount of energy, via the fragmentation yield of the molecular system.

IV. CONCLUSION AND OUTLOOK

We performed an interaction between peptides and ions at a kinetic energy corresponding to the Bragg peak, where ion beams deposit the maximum of their energy in biological matter, in order to destroy tumor cells in hadrontherapy. By means of mass spectrometry, we analyzed the cationic products of protonated collagen peptides and triple-helix models after single collisions with C^{4+}: our results show that mainly electrons are targeted, leading to nondissociative ionization, transfer of electronic energy followed by conversion into vibrational energy triggering inter- and intramolecular fragmentation. Interestingly, our results indicate that C^{4+} ions also interact with individual protons in the peptide, leading to the detachment of one of them, which has never been observed after photoabsorption. This ion-specific proton detachment increases with the number of protons, and probably induces vibrational energy transfer, similarly to ionization. This amount of energy might be varied by changing the geometrical structure and size of the molecular system: For peptides, our results show that an unfolded and larger system receives more transferred energy.

Our work shows that the main radio-induced molecular processes can be analyzed and understood experimentally by mass spectrometry techniques, but also opens up alternative perspectives by investigating the evolution of the amount of vibrational energy transferred to a biomolecular system as a function of the ion beam kinetic energy in the 0.1–100 MeV/u range.

[1] *Carbon-Ion Radiotherapy: Principles, Practices, and Treatment Planning*, edited by H. Tsujii, T. Kamada, T. Shirai, K. Noda, H. Tsuji, and K. Karasawa (Springer Japan, Tokyo, 2014).

[2] *Radiation Damage in Biomolecular Systems*, edited by G. Garcia Gómez-Tejedor and M. C. Fuss (Springer Netherlands, Dordrecht, 2012).

[3] J. de Vries, R. Hoekstra, R. Morgenstern, and T. Schlathölter, Phys. Rev. Lett. **91**, 053401 (2003).

[4] E. Alizadeh, T. M. Orlando, and L. Sanche, Annu. Rev. Phys. Chem. **66**, 379 (2015).

[5] R. H. Duncan Lyngdoh and H. F. Schaefer, Acc. Chem. Res. **42**, 563 (2015).

[6] K. B. Bravaya, E. Epifanovsky, and A. I. Krylov, J. Phys. Chem. Lett. **3**, 2726 (2012).

[7] H. W. Jochims, M. Schwell, H. Baumgärtel, and S. Leach, Chem. Phys. **314**, 263 (2005).

[8] J.-C. Poully, J. Miles, S. De Camillis, A. Cassimi, and J. B. Greenwood, Phys. Chem. Chem. Phys. **17**, 7172 (2015).

[9] E. P. Mansson, S. De Camillis, M. C. Castrovilli, M. Galli, M. Nisoli, F. Calegari, and J. B. Greenwood, Phys. Chem. Chem. Phys. **19**, 19815 (2017).

[10] S. Maclot, R. Delaunay, D. G. Piekarski, A. Domaracka, B. A. Huber, L. Adoui, F. Martin, M. Alcami, L. Avaldi, P. Bolognesi, S. Diaz-Tendero, and P. Rousseau, Phys. Rev. Lett. **117**, 073201 (2016).

[11] S. Ptasinska, P. Candori, S. Denifl, S. Yoon, V. Grill, P. Scheier, and T. D. Märk, Chem. Phys. Lett. **409**, 270 (2005).

[12] J.-W. Shin and E. R. Bernstein, J. Chem. Phys. **140**, 044330 (2014).

[13] H. W. Jochims, M. Schwell, J. L. Chotin, M. Clemino, F. Dulieu, H. Baumgärtel, and S. Leach, Chem. Phys. **298**, 279 (2004).

[14] S. Bari, P. Sobocinski, J. Postma, F. Alvarado, R. Hoekstra, V. Bernigaud, B. Manil, J. Rangama, B. Huber, and T. Schlathölter, J. Chem. Phys. **128**, 074306 (2008).

[15] S. Maclot, D. Grzegorz Piekarski, A. Domaracka, A. Mery, V. Vizcaino, L. Adoui, F. Martin, M. Alcami, B. A. Huber, P. Rousseau, and S. Diaz-Tendero, J. Phys. Chem. Lett. **4**, 3903 (2013).

[16] S. Denifl, I. Maehr, F. F. da Silva, F. Zappa, T. D. Märk, and P. Scheier, Eur. Phys. J. D **51**, 73 (2009).

[17] B. Puschnigg, S. E. Huber, P. Scheier, M. Probst, and S. Denifl, Eur. Phys. J. D **68**, 119 (2014).

[18] M. Dey and J. Grotemeyer, Eur. Mass Spectrom. **1**, 95 (1995).

[19] D. Ghosh, A. Golan, L. K. Takahashi, A. I. Krylov, and M. Ahmed, J. Phys. Chem. Lett. **3**, 97 (2012).

[20] S. Ptasinska, S. Denifl, P. Scheier, and T. D. Märk, J. Chem. Phys. **120**, 8505 (2004).

[21] J.-C. Poully, V. Vizcaino, L. Schwob, R. Delaunay, J. Kocisek, S. Eden, J.-Y. Chesnel, A. Méry, J. Rangama, L. Adoui, and B. Huber, ChemPhysChem **16**, 2389 (2015).

[22] T. Schlathölter, F. Alvarado, S. Bari, A. Lecointre, R. Hoekstra, V. Bernigaud, B. Manil, J. Rangama, and B. Huber, ChemPhysChem **7**, 2339 (2006).

[23] M. Ryszka, R. Pandey, C. Rizk, J. Tabet, B. Barc, M. Dampc, N. J. Mason, and S. Eden, Int. J. Mass Spectrom. **396**, 48 (2016).

[24] N. J. Kim, H. Kang, G. Jeong, Y. S. Kim, K. T. Lee, and S. K. Kim, J. Phys. Chem. A **104**, 6552 (2000).

[25] A. Giuliani, A. R. Milosavljevic, F. Canon, and L. Nahon, Mass Spectrom. Rev. **33**, 424 (2014).

[26] D. Egorov, L. Schwob, M. Lalande, R. Hoekstra, and T. Schlathölter, Phys. Chem. Chem. Phys. **18**, 26213 (2016).

[27] O. Gonzalez-Magana, M. Tiemens, G. Reitsma, L. Boschman, M. Door, S. Bari, P. O. Lahaie, J. R. Wagner, M. A. Huels, R. Hoekstra, and T. Schlathölter, Phys. Rev. A **87**, 032702 (2013).

[28] S. Martin, C. Ortega, L. Chen, R. Brédy, A. Vernier, P. Dugourd, R. Antoine, J. Bernard, G. Reitsma, O. Gonzalez-Magaña, R. Hoekstra, and T. Schlathölter, Phys. Rev. A **89**, 012707 (2014).

[29] W. D. Hoffmann and G. P. Jackson, J. Am. Soc. Mass Spectrom. **25**, 1939 (2014).

[30] S. Bari, R. Hoekstra, and T. Schlathölter, Phys. Chem. Chem. Phys. **12**, 3376 (2010).

[31] M. Lalande, C. Comby-Zerbino, M. Bouakil, P. Dugourd, F. Chirot, and J.-C. Poully, Chem. - Eur. J. **24**, 13728 (2018).

[32] R. Berisio, L. Vitagliano, L. Mazzarella, and A. Zagari, Protein Sci. **11**, 262 (2002).

[33] S. Bari, O. Gonzalez-Magaña, G. Reitsma, J. Werner, S. Schippers, R. Hoekstra, and T. Schlathölter, J. Chem. Phys. **134**, 024314 (2011).

[34] L. Schwob, M. Lalande, J. Rangama, D. Egorov, R. Hoekstra, R. Pandey, S. Eden, T. Schlathölter, V. Vizcaino, and J.-C. Poully, Phys. Chem. Chem. Phys. **19**, 18321 (2017).

[35] L. C. Tribedi, A. N. Agnihotri, M. E. Galassi, R. D. Rivarola, and C. Champion, Eur. Phys. J. D **66**, 303 (2012).

[36] S. R. Carr and C. J. Cassady, J. Mass Spectrom. **32**, 959 (1997).

[37] C. J. Cassady, J. Am. Soc. Mass Spectrom. **9**, 716 (1998).

[38] B. A. Budnik, Y. O. Tsybin, P. Hakansson, and R. A. Zubarev, J. Mass Spectrom. **37**, 1141 (2002).

[39] A. R. Milosavljevic, F. Canon, C. Nicolas, C. Miron, L. Nahon, and A. Giuliani, J. Phys. Chem. Lett. **3**, 1191 (2012).

[40] L. Schwob, M. Lalande, D. Egorov, J. Rangama, R. Hoekstra, V. Vizcaino, T. Schlathölter, and J.-C. Poully, Phys. Chem. Chem. Phys. **19**, 22895 (2017).

[41] J. F. Ziegler, J. Appl. Phys. **85**, 1249 (1999).